THE IBIS TELESCOPE: SCIENTIFIC OBJECTIVES

F. LEBRUN
(On behalf of the IBIS consortium)

DAPNIA, Service d'Astrophysique
CEA-Saclay, 91191 Gif-sur-Yvette Cedex, France

The IBIS gamma-ray telescope onboard the ESA INTEGRAL satellite will begin its observing programme by the end of the year. Its high angular resolution (12'), high sensitivity (mCrab level) and precise timing (0.1 ms) are particularly well adapted to the study of the galactic and extragalactic accretion powered sources. Weekly scans of the galactic disc will allow the detection of transient sources that may be considered as targets of opportunity. The spectral performance of IBIS (10% at 60 keV) will allow also the study of line emission from SNRs (^{44}Ti), pulsars (cyclotron lines) and X-ray novae. The polarimetric capabilities of the telescope may also give new insights into the gamma-ray burst phenomenon.

1 The INTEGRAL mission

The INTEGRAL astrophysical observatory will be launched from Baïkonour in October 2002 for a 5 -year mission [1]. This 2nd medium size ESA project is devoted to the observation of the gamma-ray sky between 3 keV and 10 MeV. With regard to its predecessors, such as GRANAT or the COMPTON observatory, it offers drastically improved performances in spectroscopy and imaging. This is achieved with the use of two specialised coded-aperture instruments. The spectrometer SPI [2], using the cooled germanium spectroscopy, has got very high spectroscopic capabilities with an improved sensitivity over a very wide field of view (~ 25° FWHM). The imager, IBIS whose science prospects are presented here, uses two pixel gamma-cameras to achieve performances incredibly improved with regard to GRANAT/SIGMA in all aspects: angular resolution, sensitivity, energy range, spectral resolution, field of view and timing. Two third of the INTEGRAL observing time is open to the international science community while the guaranteed time is used by INTEGRAL science team to perform what is called the core programme. This programme is aimed at providing a weekly monitoring of the accessible part of the Milky-Way to reveal bursts of activity, such as the X-ray novae, and on a long term to build a Galactic map both in radionuclide lines and in the continuum.

2 The IBIS Telescope

The basic IBIS concept is similar to SIGMA that used the coupling between a fixed tungsten coded mask and a gamma camera. The main differences are in the detectors. The IBIS detection unit is made not with one but with two superimposed gamma cameras. Detectors in space are affected for some time after the passage of charge particles such as cosmic-ray protons. On a very large detector such as the SIGMA gamma camera that is crossed several times per millisecond, the overall performances, and particularly the spatial resolution, are degraded at low energy. Pixel gamma-cameras where each pixel is an independent detector with its own electronic chain avoid this problem. In that case, the detectors are so small that they do not even see one proton per second. Moreover, the angular resolution of pixel gamma cameras is independent of energy and can be made as good as permitted by the power consumed and dissipated by the large number of electronic chains. It is difficult with a single detector and its electronic chain to cover more than two decades in energy. For that reason, the IBIS detection unit uses two cameras, ISGRI covering the range from 15 keV to 1 MeV

and PICsIT covering the range from 170 keV to 10 MeV. Using 128x128 CdTe semi-conductors operating at ambient temperature, ISGRI offers 4.6 mm spatial resolution and 8% energy resolution at 122 keV. With 64x64 CsI scintillators coupled to Si photodiodes, the spatial resolution of PICsIT is 9.2 mm and its spectral resolution attains 12% at 662 keV. The time at which an interaction occurs in one or the other camera is encoded with high precision allowing the establishment of coincidences within a few microseconds between the two cameras. The "Compton mode" will take advantage of these events in coincidence. To reduce the internal background mainly due to the cosmic-ray protons, both cameras are surrounded by a 2 cm thick BGO detector readout by photomultipliers. This VETO system can be used in part or globally in anticoincidence with the cameras. Passive shields are used to reduce the low energy background due to celestial photons outside the field of view. The hopper, a sort of hollow truncated tungsten pyramid, 1 mm thick, 55 cm high, have its faces in the planes joining the detector edges to the mask edges. In addition, the carbon fibre structure supporting the mask is covered with thin lead foils.

The one square-meter tungsten mask is 1.6 cm thick providing a stopping power of 72% at 2 MeV. The mask support structure opacity has been minimised, attaining 50% at 20 keV. Its basic pattern is a MURA with 53x53 square elements of 11.2 mm by side. Placed 3.1 m above the detection unit, this mask offers an angular resolution of 12' and a field of view of 19°x19° at half sensitivity. The resulting localisation accuracy for a bright source is limited by the spacecraft attitude restitution to 20 arcsec.

Possible drifts in the detector response can be tracked thanks to a tagged source of ^{22}Na that produces radioactive lines at 511 and 1275 keV and induces W and Pb fluorescence lines at 60 and 75 keV in the passive shields. Depending on the detector characteristics, telemetry limitations have imposed different ways to transmit the data. All the information relative to every ISGRI detection (time, detector address, pulse height, pulse rise-time) is transmitted to the ground. While a specific mode allow to do the same with PICsIT events, it is anticipated that the PICsIT count-rate will imposed most of the time the use of an histogramming mode. In the spectral-imaging mode, images in each energy channel are built on board and transmitted to the ground. The accumulation time could be of the order of a several minutes to a few hours. In the spectral timing mode, spectra are accumulated over times as short as one millisecond. The use of these modes will depend on the actual background in orbit. Similarly to the ISGRI events, all the information relative to the triggers in coincidence between ISGRI and PICsIT will be transmitted to the ground. However, here again, it is anticipated that they could overflow the telemetry. To avoid this, an on board software, considering the interaction positions and energy deposits, discards the events that could not have passed through the IBIS mask. This selection reduces by a factor of four the background and the telemetry rate required by the Compton mode events.

At the beginning of the mission the background on the ISGRI detector is expected to be around 700 s^{-1} but due to the lowering of the solar activity, it may reach 1000 s^{-1} five years later. Taking into account the detection efficiency, the imaging efficiency and the mask support- structure opacity, the 2621 cm^2 of ISGRI should result in a continuum sensitivity at 100 keV of 5 10^{-7} cm^{-2} s^{-1} keV^{-1} while the sensitivity to narrow lines is around 2 10^{-5} cm^{-2} s^{-1}. Similarly, the cumulated sensitivity of PICsIT and the Compton mode is about 2 10^{-7} cm^{-2} s^{-1} keV^{-1} at 1 MeV for the continuum and 4 10^{-5} cm^{-2} s^{-1} for narrow lines.

Table 1

Scientific performance parameters	SIGMA	IBIS
Energy range (keV)	40-1300	15-8000
Angular resolution (arcmin)	18	12
Spectral resolution at 100 keV	15 %	8 %
Field of view (50 % coding)	9.4° × 9.7°	19° × 19°
Timing accuracy	4 s	100 µs
Broad-band sensitivity ($\Delta E=E/2$, 3 σ, 10^6 s) at 100 keV (cm^{-2} s^{-1} keV^{-1})	10^{-5}	5 10^{-7}
Broad-band sensitivity ($\Delta E=E/2$, 3 σ, 10^6 s) at 1 MeV (cm^{-2} s^{-1} keV^{-1})	10^{-5}	2 10^{-7}

Table 1 summarizes the key performance parameters of IBIS in comparison with SIGMA. The huge gain in sensitivity is not obtained at the expense of any other parameter. In particular, to avoid source confusion, it was essential to maintain the angular resolution. This sensitivity gain together with the enlarged field of view and spectral coverage will certainly result in the detection of hundreds of new galactic and extragalactic sources. This is illustrated in Figure 1 that displays a simulation of a one-day observation of IBIS toward the galactic centre.

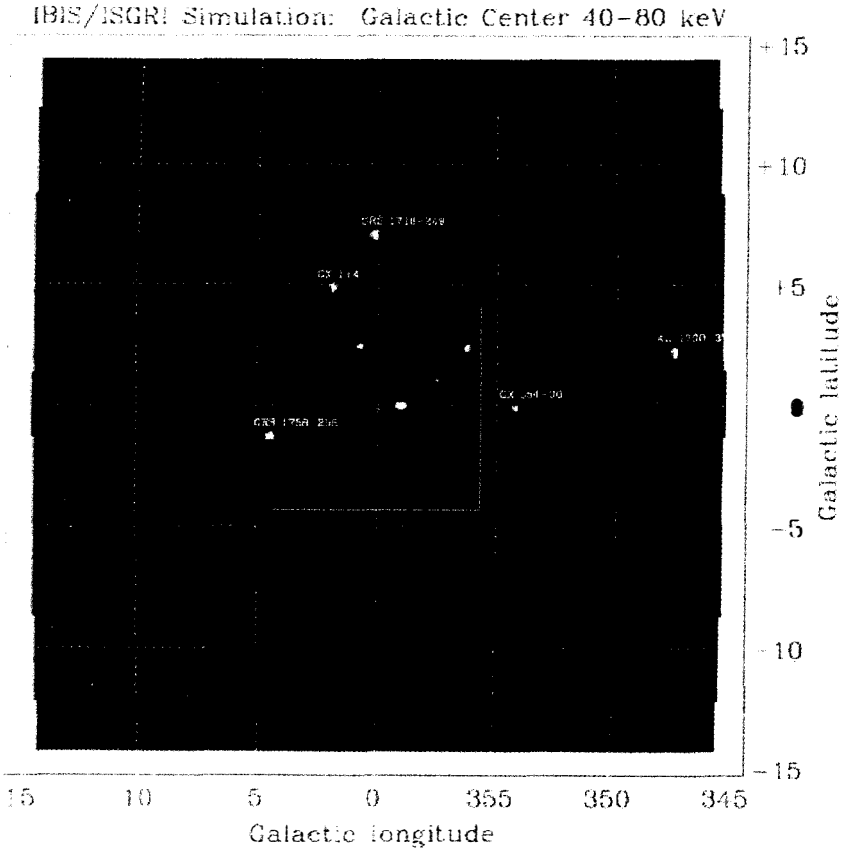

Figure 1 : Simulation of an IBIS observation pointed at the Galactic centre. The white square represents the fully coded field of view.

It is not possible to address in this paper all the topics where IBIS will make progress and the past teaches us that it is probably hopeless to predict the main outcome of the IBIS observations. However, on the basis of the IBIS performance, one can pinpoint some of the areas where surely significant progresses will be made.

3 IBIS Science Prospects

3.1 Galactic Sources

3.1.1 Accreting black holes

Spectra of accreting black holes in all their states show a non-thermal high-energy tail. In the classical interpretation, this emission results from the comptonisation of soft photons emitted by the external part of

the accretion disc by the hot electrons of the inner disc [3]. This model predicts a cut-off energy around a few hundred keV. However the Cygnus X-1 spectrum seems to extend to higher energies, possibly above 1 MeV [4]. Several models predict a higher cut-off energy, up to 400 keV [5], or above [e.g. 6,7]. In this context, precise spectral/imaging measurements above 600 keV are essential. This can be achieved with IBIS not only in the case of Cygnus X-1, but also on weaker sources such as 1E1740.7-2942.

The Rossi XTE satellite has observed the temporal behaviour of many black hole candidates. It has detected high frequency Quasi Periodic Oscillations which can be directly related to the events taking place very close to the black hole horizon, as the inverse of their frequency is close the horizon crossing time $t = r_h / c$ (r_h being the horizon radius)[8,9]. With its 0.1 ms timing resolution, IBIS will be able to monitor these oscillations from medium and high mass black hole, with masses above around 20 solar masses, characteristic of microquasars, for instance. It will give also insight to hydrodynamical phenomena occurring a bit further from the horizon, such as, for instance, the radial instabilities close to the accretion-disk inner edge, or in the centrifugal barrier area [10]. On the other hand, IBIS observations of low frequency QPOs will enable us to study the accretion disk global behaviour.

If all X-ray novae have similar peak luminosities in the 40-150 keV range [11] (~ 10^{37} erg s^{-1}), IBIS will detect all of them and they may become targets of opportunity if they are bright enough (> 500 mCrab). Transient high-energy lines have been observed by SIGMA in the spectra of Nova Musca [12] and 1E1740.7-2942 [13]. Considering the wider field of view of IBIS, that is always an advantage to pick up transient phenomena, and the drastic improvement in sensitivity, one can expect several such detections in particular in the course of the Galactic central radian survey.

3.1.2 Accreting neutron stars

Neutron stars will be objects of prime interest for IBIS. The spectral difference between accreting neutron stars or black holes can undoubtedly be better seen with the improvement in sensitivity and spectral coverage. Thanks to its large field of view, there is no doubt that a large number of X-ray bursters will be found especially in the Galactic bulge.

In a dozen of cases, cyclotron lines have been observed in the spectra of accreting pulsars. These detections are particularly useful since they provide a direct measurement of the magnetic field strength. The IBIS sensitivity and spectral resolution below 100 keV lead us to expect many more detections and the measurements of higher harmonics. This is illustrated in Figure 2 where the parameters extracted from the BeppoSAX observation of X0115+63 [14] have been used to predict an IBIS observation. In this simulation of a 10^5 s observation, the second, third and fourth harmonics are clearly visible. So far 44 accretion powered pulsars have been found. The number of known transients is more than twice the number of persistent pulsars, 30 versus 14. This is very encouraging for the both the Galactic Plane Survey and the Galactic Centre Deep Exposure.

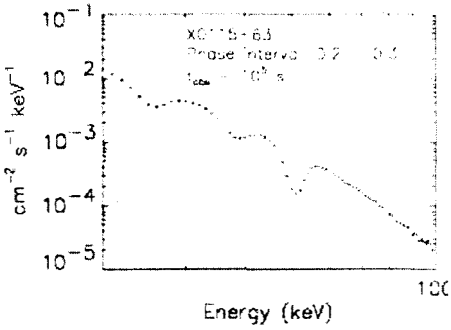

Figure 2

3.1.3 Galactic Centre Region

The star motions in the vicinity of Sgr A* imply a mass of 3 10^6 $M_\odot$ for the central object, most likely a supermassive black hole. However, despite 10^7s spent in observing the Galactic Centre, SIGMA failed to detect any emission from SgrA* [15]. Specific accretion models were proposed to account for this apparent lack of high-energy activity from Sgr A. A single day of IBIS observations toward the Galactic center will provide a better sensitivity than that attained after several years by SIGMA. During the INTEGRAL core programme, INTEGRAL will point at the Galactic centre for 10^6 s every year and open time proposals will certainly increase very significantly this figure so that the achieved sensitivity may be several ten times below the SIGMA upper limit in the direction of Sgr A*.

A comparison of the galactic continuum emission at 100 keV measured by OSSE in the galactic center direction and the total flux of the sources measured by SIGMA [16] suggested that most of this emission

could be diffuse in nature. However, nor an Inverse Compton origin, nor the bremsstrahlung seems a tenable interpretation since the implications on the electron spectrum are in conflict with other observations or require a huge power [17]. The spectral shape of this unresolved component is very similar to that of the accreting black holes in their low (hard) state so that it seems likely that point sources below the SIGMA detection threshold may contribute significantly [18]. Thanks to its imaging performance and its very good sensitivity, IBIS should provide a clear-cut answer regarding the genuine nature of this emission.

3.1.4 Line and Continuum Emission from shell-type Supernova Remnants

Supernova remnants, individually or in superbubbles [19], are probably the source of Galactic cosmic-rays. While the detection of high energy gamma-rays resulting from accelerated protons is still under debate [20, 21], non-thermal X-ray and TeV gamma-ray emission have been detected in three shell-type SNRs giving confidence in the electron synchrotron and inverse-Compton emission interpretation. In addition to measurements over a wider energy range of the already measured non-thermal tails, IBIS will certainly provide detections of non-thermal emission from some other SNRs.

Detection of ^{44}Ti lines from Cas A [22, 23] opens new possibilities to study the nucleosynthesis and detect new hidden young SNRs. The IBIS sensitivity and spectral performance should permit a breakthrough in this domain. Measurements of the low energy lines at 68 and 78 keV from historical SNRs should permit much more precise estimates of the ^{44}Ti yield. While it is estimated that ~3 supernovae should occur per century in the Milky-Way, none was observed in the last 3 centuries suggesting that most of them occurred in highly absorbed regions. If this is the case, the IBIS sensitivity should allow the detection of all supernovas that occurred in the past century and some of the older.

3.1.5 Line and Continuum Emission from Classical Novae

Due to the opacity of the expanding material in the early phases, the optical detection of a nova happens a few days after the explosion. On the other hand, the gamma-ray emission results from a competition between the ^{18}F (τ ~15 mn) and ^{13}N (τ ~ 2 hours) decay and the decreasing opacity of the envelope. As a result, the lines and the Compton continuum appear a few hours after the explosion. With the exception of a very nearby nova, the rapid decay would not allow the detection of the nova in gamma-rays after an optical alert. However, according to the model of Hernanz et al. [24], IBIS can detect the 100 keV continuum emission of a 8 kpc distant ONe nova during the first 6 hours (5.5 kpc for a CO nova) . Due to the large field of view of IBIS, one may therefore expect several serendipitous detections over a 5 year-mission, the nearest allowing also the detection of the annihilation line.

3.2 Extragalactic sources

3.2.1 Active Gactic Nuclei

A main result of recent CGRO observations is the discovery that the broad band continuum of AGNs strongly depends on their type. IBIS will clarify the details of this dependence with a program of systematic observations of a significant number of objects within the different classes. The outcome will undoubtedly have a major impact on production mechanism identification, on Unified Theories of AGNs and on our understanding of the composition of the Cosmic Diffuse Background. Here we briefly outline the potential of IBIS in such studies. At low energies these are mostly radio quiet objects such as Seyferts of various types. Although it is known that in these AGNs the spectrum fall off above 50 keV or so, the details of this cut-off are still highly uncertain mainly due to difficulties in fitting complex models over a limited energy band; furthermore, it is still unanswered the question of whether the spectrum is different among the various Seyfert classes. Due to its broad band coverage, IBIS will be particularly suited for the study and definition of the high energy spectral shape of this type of AGNs; we expect that over 200 Seyfert type objects will be visible by IBIS above the 5 sigma level up to 100 keV in a 1-day exposure; 20 objects can be detected up to 500 keV, allowing spectral studies to be performed on a quite large sample of sources. At higher energies, the main observation targets will be Blazar type sources like those detected by EGRET. These are sources whose spectra extend to MeV energies but due to their greater distances they are generally dimmer than Seyferts. In this case the main interest is a determination of the spectral characteristics (i.e. break) in the MeV band. To this end observations will have to be longer (typically 10^6 sec) and consequently we expect to study a limited number (10) of objects. However, it is worth noting that from these longer exposures one may expect to detect as a by-product a number of serendipitous sources, typically 4 sources per field.

3.2.2 *Gamma-Ray Bursts*

IBIS should detect gamma-ray bursts at a rate close to one per month. Having no on-board trigger, there are a priori no GRB selection on duration and super-long bursts can be detected. At the other end, the precise IBIS timing (0.1 ms) allows the detection of sub-millisecond bursts [25]. If observed, a sub-millisecond variability would be a severe constraint on the GRB models. The accuracy of the localization (20 arcsec to a few arcmin) and the rapidity of the localization and location dissemination will allow for efficient follow-up measurements. In particular the early afterglow (<1h) can be measured and afterglows from short GRBs can be searched for. The IBIS energy range (15 keV-1 MeV) is optimal for GRBs studies, allowing to build an unbiased E_{peak} distribution and the observation of X-ray flashes. The IBIS sensitivity will permit the detection of bursts more distant than $z = 15$ that are not accessible neither with HETE 2 nor with Swift [26].

3.2.3 *Clusters of Galaxies*

Recent RXTE and BeppoSAX [27,28,29,30] measurements revealed the presence of non-thermal spectral components in the spectra of four clusters of galaxies with extended regions of radio emission. While the origin of this non-thermal emission is not established, it is expected to result from the inverse Compton interactions of relativistic electrons with the cosmic microwave background radiation. Spectral and especially imaging observations with the IBIS instrument will very likely shed light on the origin of this emission in nearby clusters.

4 References

1. W. Hermsen, these proceedings
2. J.P. Roques, These proceedings
3. R. Sunyaev and L. Titarchuk, *A&A*, **86**, 121 (1980)
4. M.L. McConnell et al., *ApJ*, **543**, 928 (2000)
5. P. Laurent and L. Titarchuk, *ApJ*, **562**, L67 (1999)
6. J. Poutanen and R. Svensson, *ApJ*, **470**, 249 (1996)
7. M. Gierlinski et al., *MNRAS*, **309**, 496 (1999)
8. M. van der Klis, *Ann. Rev.A&A*, **38**, 717 (2000)
9. T.E. Strohmayer, *ApJ*., **554**, L169 (2001)
10. S. Chakrabarti and L. Titarchuk, Ap.J., **455**, 623 (1995)
11. M. Vargas et al., *ApJ*., **476**, L23 (1997)
12. A. Goldwurm et al., *ApJ*, **389**, L79 (1993)
13. B. Cordier et al., *A&A*, **275**, L1 (1993)
14. A.Santangelo et al., *ApJ*, **523**, L85 (1999)
15. P. Goldoni etal, *Astr Lett C*, **38**, 305 (1998)
16. W.R. Purcell et al., *A&AS* **120**, 389 (1996)
17. J.G. Skibo and R. Ramaty, *A&AS,* **97**, 145 (1993)
18. F. Lebrun, et al., *Astr Lett C*, **38**, 457 (1998)
19. E. Parisot, these proceedings
20. R. Enomoto et al., Nature, **416**, 823 (2002)
21. O. Reimer et al., A&A, in press (astro-ph/0205256)
22. A. Iyudin et al., *A&A*, 284, L1 (1994)
23. J. Vink et al., *ApJ*, **560**, L79 (2001)
24. M. Hernanz et al., *ApJ*, **526**, L97 (1999)
25. D. Götz and S. Mereghetti, these proceedings
26. J. Gorosabel, *4th Integral Workshop « Exploring the Gamma-Ray Universe », Alicante, ESA-SP* **459**, 419 (2000)
27. D.E. Gruber and Y. Rephaeli, *ApJ*, **565**, 877 (2001)
28. J.S. Kaastra et al., *ApJ,* 519, L119 (2000)
29. R. Fusco-Femiano et al., *ApJ*, 513, L21 (1999)
30. Fusco-Femiano, R., et al. ApJ 534, L7 (2000)